Chemistry Europe
European Chemical Societies Publishing

WILEY VCH

Excellence in Chemistry Research

Announcing our new flagship journal

- Gold Open Access
- Publishing charges waived
- Preprints welcome
- Edited by active scientists

Meet the Editors of *ChemistryEurope*

Luisa De Cola
Università degli Studi di Milano Statale, Italy

Ive Hermans
University of Wisconsin-Madison, USA

Ken Tanaka
Tokyo Institute of Technology, Japan

Chemistry–A European Journal
Research Article
doi.org/10.1002/chem.202302661
Chemistry Europe
European Chemical Societies Publishing
www.chemeurj.org

Hot Paper

Special Collection

Iron(II) Complexes of P_3-Chain Ligands: Structural Diversity

Tamás Holczbauer,[a] Dalma Gál,[b] János Rohonczy,[c] Eberhard Matern,[d] Ewald Sattler,[d] Petra Bombicz,[e] Zsolt Kelemen,*[b] and Ilona Kovács*[b]

Dedicated to Prof. Evamarie Hey-Hawkins, Prof. Manfred Scheer, and Prof. Werner Uhl.

Iron(II) complexes containing ligands with a $R_2P–P–PR_2$ unit were synthesized by metathesis reactions. With R = *t*Bu, a mixture of two isomers is formed; in one of them, the terminal phosphorus binds to the Fe center (ylidic structure), while in the other one, the central P atom is linked to Fe. Starting from differently functionalized parent triphosphanes and corresponding functionalized Fe complexes, the ratio of isomers does not change. The outcome of the reaction and therefore the binding modes of the triphosphane ligands in the resulting compounds can be influenced by the size of the substituents. In the case of R = *i*Pr a chelate complex is formed (both terminal P atoms are linked to the Fe center). Applying the mixed-substituted triphosphane, the ylidic structure of the resulting complex is preferred. The new compounds were characterized by NMR spectroscopy in solution and single-crystal X-ray diffraction in solid-state. The synthetic work was supported by DFT calculations.

Introduction

The first neutral phosphinidene-phosphorane, $CF_3P{=}PMe_3$, was prepared by Burg and Mahler by reaction of the cyclophosphanes $(CF_3P)_4$ or $(CF_3P)_5$ with excess PMe_3.[1] These low-valent organic $RP{=}PR_3$ ylides can be interpreted as phosphinidenes protected by phosphanes (PR_3). They can be considered as phosphorus analogues of Wittig reagents, which was demonstrated by reactions with aldehydes that generate phosphaalkenes RP=CH(R).[2]

Earlier studies of the Fritz group on silylphosphanes led to phosphanyl-substituted phosphorus rich phosphinidene-σ^4-phosphoranes $R_2P–P{=}PR_3$. The first example was $tBu_2P–P{=}P(tBu_2)Br$ (**1**),[3] which was formed from the reaction of lithium triphosphanide $[tBu_2P–P–PtBu_2]Li(THF)_2$ (**2**) and 1,2-dibromoethane. Later, it was demonstrated that the substituents at the terminal P atoms of the triphosphanide strongly influence the formation of the phosphinidene-phosphoranes. In the presence of *t*Bu substituents, the corresponding ylide is the main product and only trace amounts of $tBu_2P–P(Br)–PtBu_2$ can be detected, while substituents such as *i*Pr, Ph, NEt_2 favor the formation of the isomeric triphosphanes $R_2P–P(X)–PR_2$ (X=Br, Me).[4] The presence of the reactive halogen on the phosphorane phosphorus atom in $tBu_2P–P{=}P(tBu_2)Br$ (**1**) allows a metathesis reaction with R′Li (R′ = Me, *n*Bu) to form $tBu_2P–P{=}P(tBu_2)R'$ and $tBu_2P–P(R')–PtBu_2$.[5] For steric reasons, the formation of the ylide is preferred in the case of the less bulky methyl group, whereas the isomeric triphosphane is mainly formed with *n*BuLi. The similar reaction of **1** with $LiPR''_2$ (R″ = Me, $SiMe_3$) leads to *iso*-tetraphosphanes $(tBu_2P)_2P–PR''_2$, and the formation of the corresponding ylide was not detected.[5] Besides the *iso*-tetraphosphanes, diphosphanes $R''_2P–PR''_2$ appeared in the reaction mixture, which can be attributed to a Li/Br exchange between **1** and $LiPR''_2$ and subsequent reaction of $BrPR''_2$ with $LiPR''_2$. In the Li/Br exchange reaction, $tBu_2P–P{=}P(tBu_2)Li$ might be expected as an intermediate, but the presence of $[tBu_2P–P–PtBu_2]Li(THF)_2$ (**2**) was verified with the aid of ^{31}P NMR spectroscopy. In turn, **2** can form *iso*-tetraphosphanes with $BrPR''_2$. (Reactivity of **1** was summarized in Scheme S1 in Supporting Information.)

Ylide **1** shows remarkable synthetic potential as a phosphinophosphinidene ($tBu_2P–P$) transfer agent. Numerous deriva-

[a] Dr. T. Holczbauer
Centre for Structural Science and Institute for Organic Chemistry
HUN-REN Research Centre for Natural Sciences
Magyar Tudósok körútja 2, 1117 Budapest (Hungary)
[b] D. Gál, Dr. Z. Kelemen, Dr. I. Kovács
Department of Inorganic and Analytical Chemistry
Budapest University of Technology and Economics
Műegyetem rkp. 3. 1111 Budapest (Hungary)
E-mail: kovacs.ilona@vbk.bme.hu
kelemen.zsolt@vbk.bme.hu
Homepage: http://iaachem.bme.hu
[c] Dr. J. Rohonczy
Department of Inorganic Chemistry
Institute of Chemistry, Eötvös Loránd University
Pázmány Péter sétány 1/A, Budapest, 1117 (Hungary)
[d] Dr. E. Matern, Dr. E. Sattler
Institute of Inorganic Chemistry
Karlsruhe Institute of Technology (KIT)
Engesserstr. 15, 76131 Karlsruhe (Germany)
[e] Dr. P. Bombicz
Centre for Structural Science
HUN-REN Research Centre for Natural Sciences
Magyar Tudósok körútja 2, 1117 Budapest (Hungary)

Supporting information for this article is available on the WWW under https://doi.org/10.1002/chem.202302661

Special Collection Part of a Special Collection on the p-block elements.

tives of it can be prepared by exchange with other phosphanes (e.g. PEt_3, PPh_3, $P(NEt_2)_3$).[6] **1** and $tBu_2P{-}P{=}P(tBu_2)Me$ are known to be able to transfer the $tBu_2P{-}P$ unit to the metal centers in reactions involving transition metal complexes.[7] On the other hand only a few examples are known for a complex formation without P–P cleavage. We were the first, who prepared such a complex with side-on coordination (Figure 1, $R^1{=}R^2{=}tBu$ [ML]=Pt(PPh_3)Br) in the reaction of **1** with $(Ph_3P)_2Pt{\cdot}C_2H_4$ or $Pt(PPh_3)_4$.[8] It seems that the oxidative addition (formation of a Pt–Br bond) is faster than any decomposition reactions which would lead to the formation of the corresponding phosphino-phosphinidene ($tBu_2P{-}P$). Interestingly, the same coordination mode with different metal centers (Pt, Pd, Ni, W, Mo) can be achieved by a different synthetic protocol as it was demonstrated by Pikies and Grubba.[9–12] These complexes exhibit similar bonding situations, as a common motif the two P–P bonds in the molecule differ significantly. One of the P–P bonds is between 2.22–2.24 Å (typical for P–P single bonds), while the other one is somewhat shorter (2.13–2.16 Å), indicating some double bond character. It is noteworthy, that the metal–phosphorus bonds are more equalized in case of M=Mo and W, while in case of Pt, Pd and Ni the bond lengths between the central P and M center are more elongated.

The question arises whether other complexes with different coordination modes can be achieved. We therefore sought to investigate whether **II**, **III** and **IV** type complexes might be synthetically available. Reported herein are the results of this study, including the preparation and characterization of the new complexes. The effect of the R substituents on the complexation mode was explored and the synthetic work was supported by DFT calculations.

Results and Discussion

Complexation with the $tBu_2P{-}P{-}PtBu_2$ ligand

Earlier works focused on the complexation reaction of $R_2P{-}P{=}PR_2Br$ or the corresponding triphosphanide $[R_2P{-}P{-}PR_2]Li$ with early and late transition metals, but to the best of our knowledge, there was no attempt to investigate the corresponding iron complexes. Generally, iron shows more versatile complexation modes, due to the availability of both occupied and empty orbitals. Therefore $tBu_2P{-}P{=}P(tBu_2)Br$ (**1**) was reacted with **KFp** (**Fp**=$CpFe(CO)_2$) in toluene at −20 °C to give the isomers $tBu_2P{-}P{=}P(tBu_2)Fp$ (**3a**) and $tBu_2P{-}P(Fp){-}PtBu_2$ (**3b**) in a ratio of 1 : 1.8 (according to integration of the signals of the Cp groups in the ^1H NMR spectrum) (Scheme 1). The dimer **Fp_2** and the protonated triphosphanes $tBu_2P{-}PH{-}PtBu_2$ and $tBu_2P{-}P{=}P(tBu_2)H$ were formed as by-products. The formation of **Fp_2** has been observed previously in the reaction of Mes^*PCl_2 {$Mes^* = 2,4,6\text{-}C_6H_2(t\text{-}C_4H_9)$} with **KFp′**(**Fp′**=$Cp^*Fe(CO)_2$, $Cp^* = \eta^5\text{-}C_5Me_5$).[13] The PH-containing products result from the elimination of isobutene, a frequent side-reaction of related *t*Bu-substituted compounds.[5,14]

Since the preparation of **1** is more laborious, we were wondering whether the product might also be obtained starting from $[tBu_2P{-}P{-}PtBu_2]Li(THF)_2$ (**2**). The reaction with **FpBr** in toluene at −20 °C gave the same products with a very

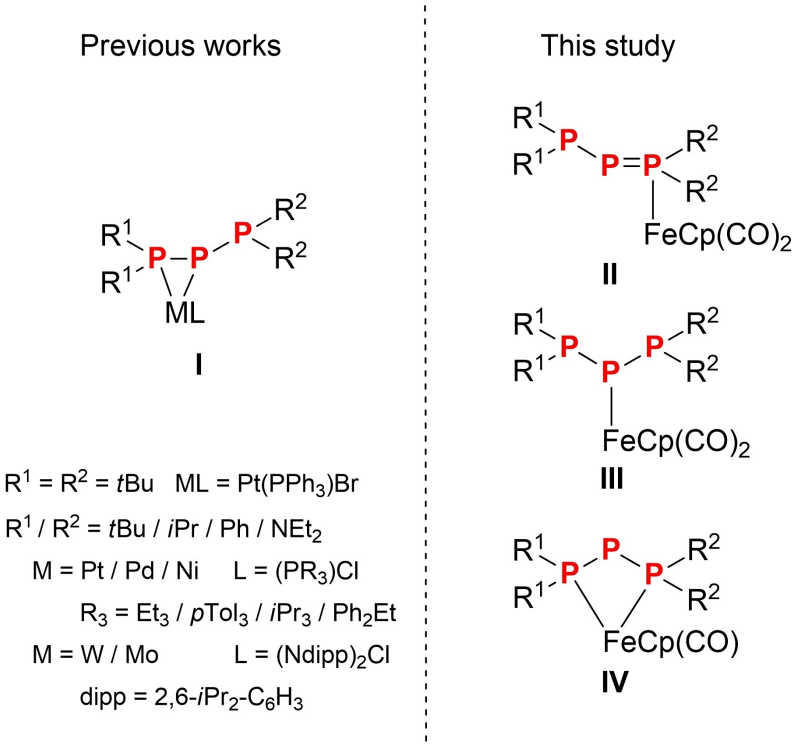

Figure 1. Schematic representation of several transition metal complexes with the $R^1{}_2P{-}P{-}PR^2{}_2$ unit in previous works[8–12] and of the Fe complexes focused in this work. Formal charges and lone electron pairs are not shown.

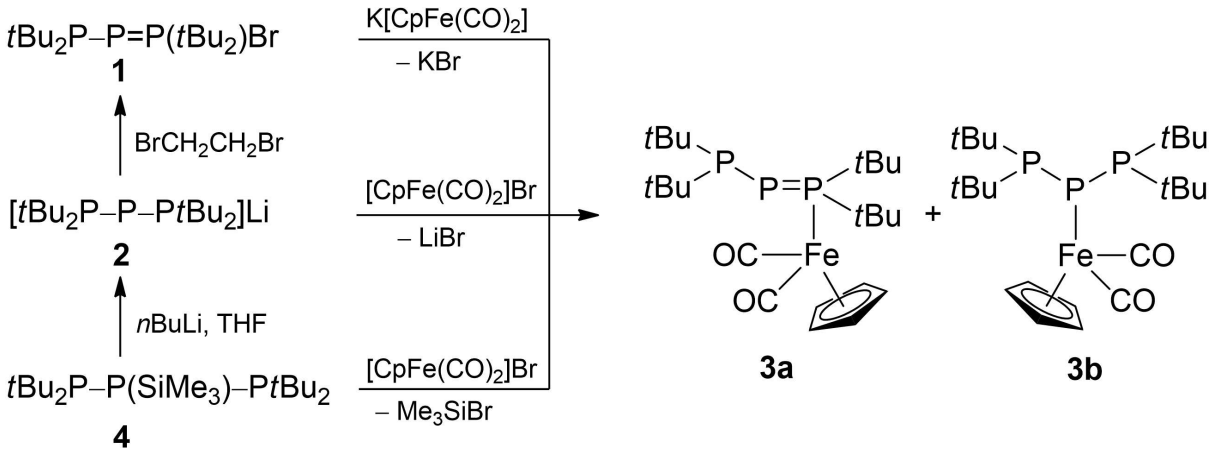

Scheme 1. Formation of the isomers **3a** and **3b**.

similar ratio of **3a**:**3b** = 1:1.9. Unfortunately, the by-products (**Fp$_2$** and PH unit containing systems) also formed. In order to prevent the formation of **Fp$_2$**, we changed the strategy. Instead of **2**, the less reactive silylated derivative *t*Bu$_2$P–P(SiMe$_3$) –P*t*Bu$_2$ (**4**) was used and reacted with **FpBr**. Applying the same reaction conditions, the reaction proceeded very slowly, **4** did not react completely even after four days according to ^{31}P NMR measurements. However, the isomers **3a** and **3b** were formed in the same ratio as in the reactions described above.

The mixture of **3a** and **3b** could be purified by recrystallization from hexane, but unfortunately any attempts (recrystallization, column chromatography) to separate them failed in our hand owing to their similar solubility and tendency for crystallization. The solid mixture of **3a** and **3b** can be stored for weeks (at room temperature and under inert atmosphere) without any significant decomposition. However, the complexes decompose slowly in solution, forming within four days *t*Bu$_2$P–PH–P*t*Bu$_2$ and **Fp$_2$** according to ^{1}H and ^{31}P NMR measurements.

The mixture of **3a** and **3b** was investigated by NMR spectroscopy in C_6D_6 solution. The ^{31}P{^{1}H} NMR spectrum shows five signal groups. The dd multiplets at −32.5 (P2), 58.2 (P3), and 104.1 ppm (P1) were assigned to **3a**. (The notation of the P atoms is consistent with that of the molecular structures obtained from X-ray measurements.) The coupling constants $^1J_{P1P2}$ = 505.8 Hz and $^1J_{P2P3}$ = 344.5 Hz are significantly different; the former value indicates a double bond character of the bond between P1 and P2 (ylidic character).[3b] The ^{31}P NMR signal of the P atom bonded to Fe in **3b** appears at −177.4 ppm as a triplet, while the broad doublet at 101.4 ppm belongs to the terminal P atoms, it is partly overlain by the P1 signal of **3a**. The unusually high coupling constant ($^1J_{PP}$ = 557.8 Hz) is remarkable for a P–P single bond. Similar high values were observed for *iso*-tetraphosphane P(P*t*Bu$_2$)$_3$[15a] and *iso*-hexaphosphane (*t*Bu$_2$P)$_2$P–P(P*t*Bu$_2$)$_2$,[15b,c] where the high coupling constants were attributed to a more planar character of the phosphorus atoms, similar to **3b**. The broad doublet signal at 101.4 ppm suggests a dynamic process in **3b**, therefore temperature-dependent ^{31}P NMR measurements were carried out (Figure S4). At 0 °C coalescence of this signal was observed, whereas at −30 °C it splits into two doublets (δ = 102.5 and 87.7 ppm, respectively), while the sharp triplet of P2 does not show any changes. The chemical shifts of P1 and P3 of **3a** do not change up to −30 °C, only the signal of P2 is shifted upfield by 30 ppm and becomes broader.

3a and **3b** cannot be separated on a preparative scale. However, suitable crystals for single crystal X-ray diffraction (SC-XRD) analysis could be selected from the crystal mixture under a microscope due to their different shapes.

3a crystallizes in the monoclinic crystal system (Figure 2, Table S6). The P1-P2 distance (2.1628(9) Å) lies slightly below the lower limit of the range of 2.17–2.24 Å given by Corbridge for P–P single bonds,[16] and indicates a small partial double bond character. The P2–P3 distance with 2.2022(9) Å lies in the range of a P–P single bond. A comparison of these data with those of the parent *t*Bu$_2$P–P=P(*t*Bu$_2$)Br (**1**) (P–P 2.202(2) Å and 2.077(2) Å, respectively)[17] shows that in **3a** the P–P bonds are more equalized. The P1–P2–P3 bond angle in **3a** measures 112.88(3)°, which is significantly larger than 105.77(7)° in **1**.

Compound **3b** crystallizes in the triclinic crystal system, with three identical molecules in the asymmetric unit (Figure 2, Table S6). The connection of the P2 atom of the ligand to the Fe center is verified and the P–Fe bond lengths lie at the upper limit of the values known from the literature (M = 2.248 Å, SD = 0.078 Å).[18] The *t*Bu$_2$P–P bond lengths are different (P1–P2 2.188(2) Å, 2.204(2) Å, 2.186(2) Å, and P2–P3 2.218(2) Å, 2.214(2) Å, 2.217(2) Å, respectively), both fall within the range of single bonds. The P1–P2–Fe1 and P3–P2–Fe1 bond angles differ significantly (128.98(8)°, 128.97(8)°, 129.87(8)°, and 107.33(7)°, 105.77(7)°, 107.09(7)°, respectively). The P–P–P bond angles also expand. The sums of the bond angles in the three molecules around P2 are 351.81(8)°, 348.90(8)°, and 351.54(8)°. Thus, P2 has a coordination geometry close to planar. The significant widening of the angles indicates the strong steric demand of the substituents.

In order to get deeper insight into the relative stability and bonding situation of **3a** and **3b** DFT calculations were performed at the ωB97X-D/Def2-TZVP level of theory. The

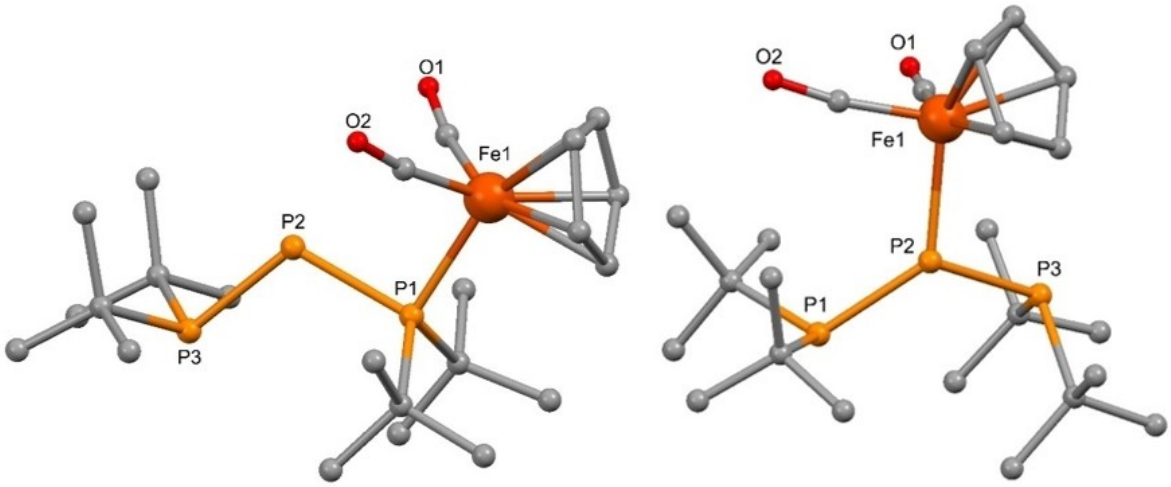

Figure 2. Molecular structures of **3a** (left) and **3b** (right). H atoms are omitted for clarity. Selected bond lengths [Å] and bond angles [°]: **3a**: P1–P2 2.1628(9), P2–P3 2.2022(9), P1–Fe1 2.3291(8), P1–P2–P3 112.88(3), P2–P1–Fe1 95.82(3), (P3–P2–P1) plane-Fe1 0.036(1); **3b**: Only one of the three molecules in the asymmetric unit is pictured here (see more details in Supporting Information). Molecule 1: P1–P2 2.188(2), P2–P3 2.218(2), P2–Fe1 2.3633(17), P1–P2–P3 115.50(8), P1–P2–Fe1 128.98(8), P3–P2–Fe1 107.33(7), (P3–P2–P1) plane-Fe1 1.076(1); Molecule 2: P1–P2 2.204(2), P2–P3 2.214(2), P2-Fe1 2.3972(17), P1–P2–P3 114.16(8), P1–P2–Fe1 128.97(8), P3–P2–Fe1 105.77(7), (P3–P2–P1) plane-Fe1 1.241(1); Molecule 3: P1–P2 2.186(2), P2–P3 2.217(2), P2–Fe1 2.3798(17), P1–P2–P3 114.58(8), P1–P2–Fe1 129.87(8), P3–P2–Fe1 107.09(7), (P3–P2–P1) plane-Fe1 1.088(1).

energy difference between the two isomers is small, **3a** is more stable by 0.4 kcal/mol. The interconversion of **3a** to **3b** might be a two-step process (Table S8 in the Supporting Information), and the barriers are around 30.0 kcal/mol, which is too high considering the applied reaction conditions. Therefore, the interconversion of these complexes is not likely. In case of **3a** Bader analysis showed that the electron density in the bond critical point is higher in case of the P2–P3 bond. The ellipticity of the electron density (0.39) demonstrates the double bond character of this bond. Investigating the Kohn–Sham molecular orbitals of **3a** it can be established that the HOMO is localized mainly at the central phosphorus atom in both cases, but polarized toward the P3 phosphorus in case of **3a**, which leads to the double bond character of the P2–P3 bond (Figure 3). The contribution of the metal fragment to the highest occupied orbitals is small, while the iron center has a significant contribution to the LUMO indicating an ionic interaction between the P_3 unit and the metal fragment. In case of **3b** the HOMO is basically the lone pair of the central phosphorus atom, similar to **3a**, but as expected, it is not polarized toward the terminal phosphorus atoms.

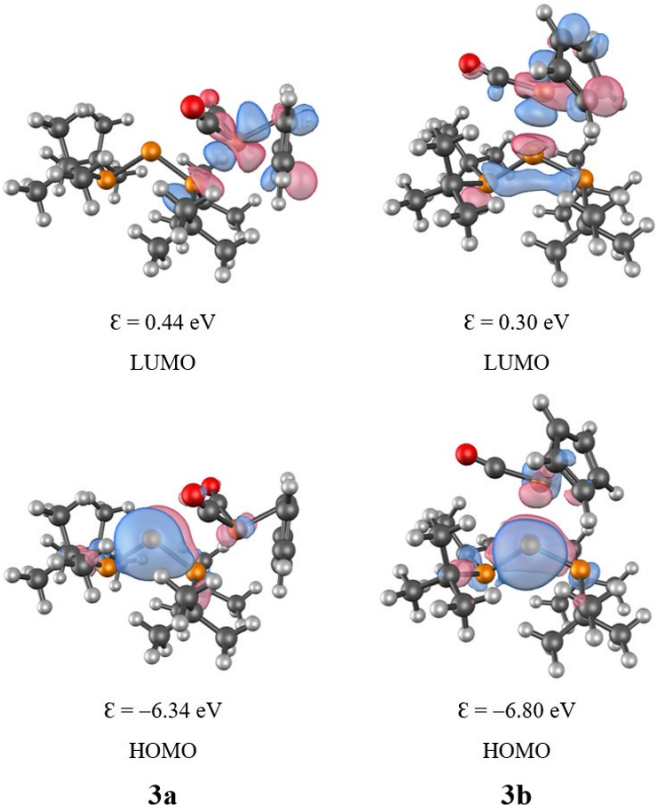

Figure 3. Kohn–Sham frontier orbitals of **3a** and **3b**.

Effect of substituents in the P_3 ligands on the binding mode

The question arises, how the binding mode might be affected when the bulky *t*Bu groups on the terminal P atoms in the P_3 unit are replaced by the less bulky *i*Pr groups.

Applying the same reaction conditions as earlier only one major product (besides by-products as for example **Fp_2**) formed in the reaction of [iPr$_2$P–P–PiPr$_2$]Li(THF)$_2$ (**5**) and **FpBr**, based on ^{31}P NMR measurements (Scheme 2). The new compound is less soluble in hexane than **Fp_2**, therefore it can be isolated in pure form after recrystallization (−30 °C). It is worth to highlight that this compound exhibits a higher thermal stability than **3a** and **3b**, it does not show any decomposition in solution even after several weeks at room temperature.

At a first glance the ^{31}P{^{1}H} NMR spectrum of **6** in C_6D_6 solution looks like an A_2M system of higher order ($\Delta\delta/J_{AM} \approx 26$).[19] However, a detailed inspection especially of the M

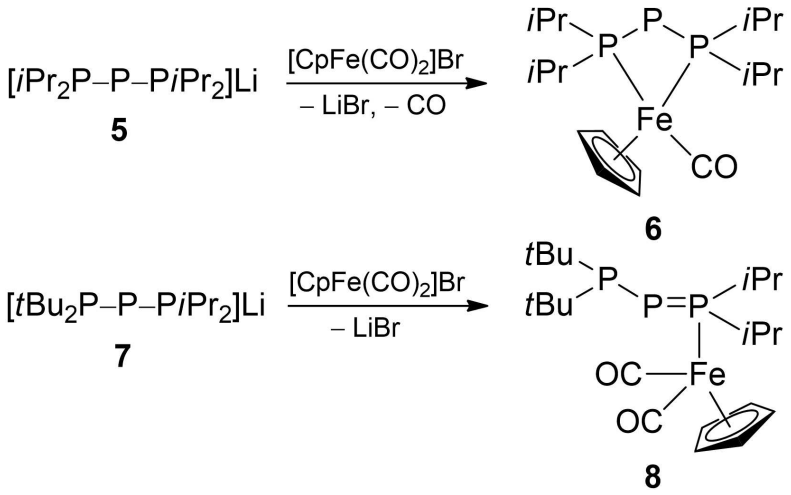

Scheme 2. Formation of complexes **6** and **8**.

multiplet gave rise to a different interpretation by DNMR. It can be established that the phosphorus atoms of the P1–P2–P3–Fe ring form an ABX spin system. The chemical shift values of the P1 and P3 terminal atoms are very similar ($\delta = 12.7$ ppm and 12.8 ppm, respectively) in agreement with the chelate structure. The $^{1}J_{PP}$ coupled dd multiplet signal of P2 ($\delta = -45.7$ ppm) has significant shoulders indicating another, minor conformer position of P2 as well. A feasible reason can be a slow flip-flop rearrangement of the P2 atom related to the P1–P3–Fe plane, similar to the dynamic ring inversion of cyclobutane. P2 is closer to the CO group in the major conformer (similar to the X-ray structure), but it can also flip to the Cp side of the mentioned plane. The phosphorus atoms of the major and minor conformers can be characterized with slightly different chemical shifts and J_{PP} coupling values. All parameters were determined with total lineshape fitting (Figure 4, details see in Supporting Information, Table S1).[20]

The 1.8–2.1 ppm methine proton region contains a pseudo nonet at 1.97 ppm (*i*Pr-A) and a septet-triplet signal at 1.87 ppm (*i*Pr-B). Both signals belong to two equivalent methine protons connected with $^{3}J_{HH}$ to their methyl protons and with $^{2}J_{HP}$ to the terminal atoms P1 and P3 and with $^{3}J_{HP}$ to P2. The ^{1}H methyl region contains two pairs of *i*Pr diastereomeric methyl signals at 1.43 and 1.11, furthermore at 1.31 and 1.04 ppm with equal six-to-six integral intensities and strange, slightly broadened quartet lineshapes. The broadening indicates an exchange between two chemically equivalent, but magnetically non-equivalent methyl group protons, where their chemical shift and $^{3}J_{HCH}$ coupling values are the same. This is in agreement with the ^{1}H{^{31}P} data. On the other hand, the $^{3}J_{HP\text{terminal}}$ and $^{4}J_{HP\text{bridge}}$ coupling values of the two conformers differ, depending on the different dihedral angles related to the P2 and P2'(bridge) phosphorus. The ring flip-flop of the phosphorus atom results in the dynamic exchange of the methyl proton couplings. All coupling parameters were determined with total lineshape fitting (Figure 3, details see in Supporting Information, Table S2–S5).[20]

The IR spectrum verifies the loss of one of the CO ligands in **6**, where only one distinct band at 1912 cm^{-1} for the CO vibration can be observed. Crystals of **6** were suitable for SC-XRD, which confirmed the chelate structure of **6** derived from NMR data as discussed before (Figure 5, Table S6). The two P–P bond lengths found in **6** are equalized (P1–P2 2.1524(11) Å and P2–P3 2.1453(10) Å, respectively) and are located at the border of single and double bond. Similar values were measured for the parent [*i*Pr$_2$P–P–P*i*Pr$_2$]Li(THF)$_2$ (**5**) (2.1627(8) Å for P1–P2 and P2–P3),[21] which also has a chelate structure. The P–Fe bond lengths are similar and lie in the range of the values known from the literature.[18] However, it should be noted that among the new compounds presented in this work, **6** shows the shortest P–Fe bond lengths. As a consequence of the chelate structure the P–P–P bond angle in **6** is strongly decreased (80.62(4)°) compared to **3a** and **3b**.

Since the outcome of the reaction was different after replacing the *t*Bu groups by *i*Pr groups, we decided to investigate the reaction of [*t*Bu$_2$P–P–P*i*Pr$_2$]Li(THF)$_2$ (**7**) with **FpBr** (Scheme 2). Similar to the reaction of **5**, only one major product was formed, but the amount of the side product **Fp$_2$** is larger. On top of that, the solubility of the new product **8** is very similar to **Fp$_2$**; even after several recrystallizations from hexane, ~15% of **Fp$_2$** remains in the product. Notably, **8** is the least thermally stable derivative among the investigated compounds, it decomposed totally within one day in solution at room temperature.

The ^{31}P{^{1}H} NMR measurements of **8** were performed in toluene-d$_8$ solution at room temperature. In the spectra, three signals with dd splitting appear at −84.1 (P2), 46.7 (P3), and 82.8 ppm (P1). The broadening of the signal of P2 suggests a dynamic process. The coupling constants $^{1}J_{P1,P2}$ (560.1 Hz) and $^{1}J_{P2P3}$ (312.0 Hz) indicate a strongly different bonding situation. The large absolute value of $^{1}J_{P1P2}$ indicates a double bond character of the bond between P1 and P2, similar to **3a**.

The molecular structure of **8** was verified by SC-XRD (Figure 5, Table S6). The structure of **8** shows high similarity to the structure of **3a**, however, both the P–P and P–Fe bond

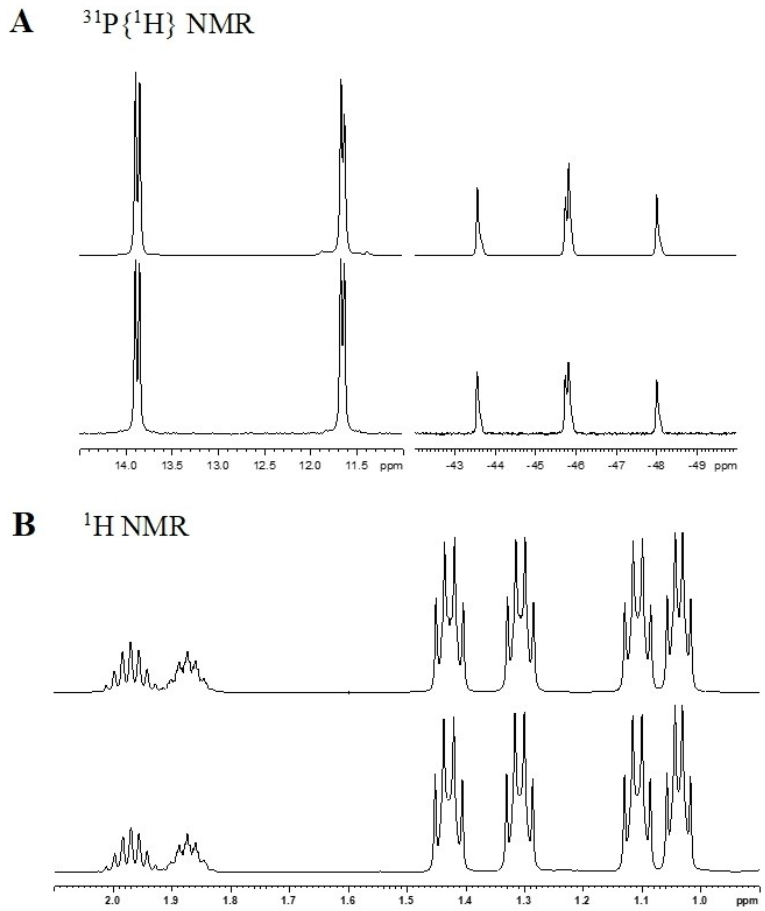

Figure 4. A: Experimental (lower), and simulated (upper) $^{31}P\{^{1}H\}$ NMR spectra (C_6D_6, 26 °C) of **6**. **B**: Experimental (lower), and simulated (upper) ^{1}H NMR spectra (C_6D_6, 26 °C) of **6**.

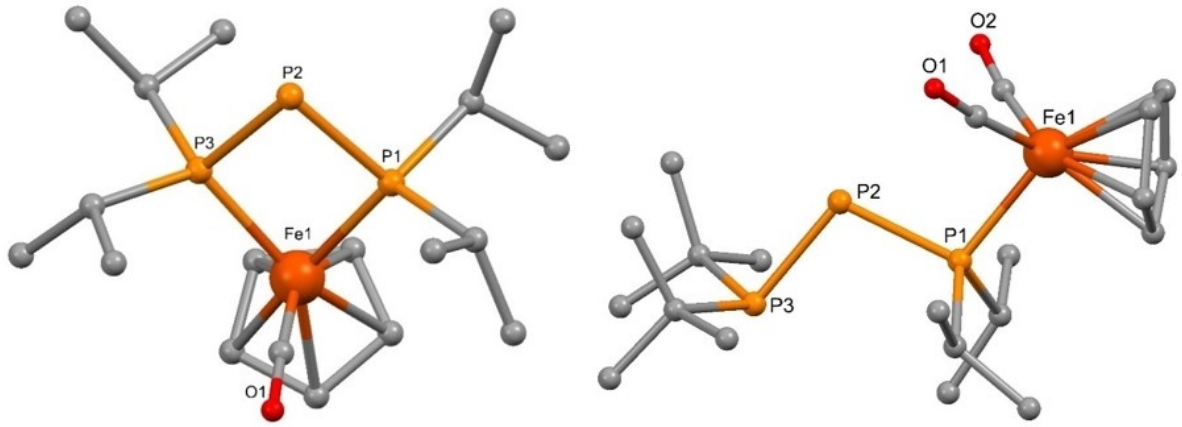

Figure 5. Molecular structures of **6** (left) and **8** (right). H atoms are omitted for clarity. Selected bond lengths [Å] and bond angles [°]: **6**: P1–P2 2.1524(11), P2–P3 2.1453(10), P1–Fe1 2.2467(8), P3–Fe1 2.2508(8), P1–P2–P3 80.62(4), P2–P1–Fe1 100.85(4), P2–P3–Fe1 100.94(4), (P3–P2–P1) plane-Fe1 0.329(1). **8**: P1–P2 2.1387(18), P2–P3 2.1899(18), P1–Fe1 2.2890(14), P1–P2–P3 104.88(7), P2–P1–Fe1 104.16(6), (P3–P2–P1) plane-Fe1 0.001(1).

lengths are shorter. The difference between the P2–P3 and P1-P2 is 0.0512(18) Å, slightly larger than in **3a**. The P–P–P bond angle in **8** is strongly decreased (104.88(7)°) compared to **3a** and **3b**. These changes result from replacing the space-demanding *t*Bu substituents on the P1 atom by *i*Pr groups.

Since the variation of the substituents on the parent P3 unit has a significant impact on the outcome of the reaction, the relative energies of the products with different complexation modes (**I**, **II**, **III**, **IV**) were investigated by DFT calculations (Table S8). In case of $R^1{=}R^2{=}$*t*Bu the relative Gibbs free energies

of **I**, **II** and **III** are very similar to each other, but the interconversion between them seems to be not possible, as the corresponding barriers are too high (above 30 kcal/mol). The energy difference between the different isomers became significant after replacing of one or two pairs of the *t*Bu substituents by *i*Pr; systems **II** and **III** are less stable than **I** by 4.6–8.7 kcal/mol. The formation of the chelate complex **IV** is exergonic in case of all investigated systems, but the thermodynamic driving force is higher in case of $R^1{=}R^2{=}i$Pr. All of these computational results are consistent with our experimental observations.

Conclusions

In this work, we have shown that the choice of the substitution pattern in the P_3 unit of $R_2P{-}P{-}PR_2$ (R = *t*Bu/*i*Pr) strongly influences the binding mode in the resulting complex compounds. Remarkably we always used the same transition metal fragment. Reactions of tBu$_2$P–P=P(*t*Bu$_2$)Br (**1**) with **KFp** (**Fp**=CpFe(CO)$_2$, Cp = η^5-C$_5$H$_5$) and [*t*Bu$_2$P–P–P*t*Bu$_2$]Li (**2**) or *t*Bu$_2$P–P(SiMe$_3$)–P*t*Bu$_2$ (**4**) with **FpBr** led to two structurally novel isomers: *t*Bu$_2$P–P=P(*t*Bu$_2$){FeCp(CO)$_2$} (**3a**) with ylidic structure and *t*Bu$_2$P–P{FeCp(CO)$_2$}–P*t*Bu$_2$ (**3b**). We could not observe the formation of a complex with a side-on coordinated P_3 ligand as known from the literature.[10,11] The ratio of isomers (approximately **3a**:**3b** = 1:1.8 based on ^{1}H NMR measurements) did not depend on the starting compounds. DFT calculations revealed that the Gibbs free energy difference between the two isomers is small, but the barrier of the interconversion is too high, therefore direct transformation between **3a** and **3b** is not likely. We also investigated the effect of the substituents in the ligands on the coordination geometry. Replacing the *t*Bu groups to the less bulky *i*Pr groups at one of the terminal phosphorus atoms leads to the formation of only the single product *t*Bu$_2$P–P=P(*i*Pr$_2$){FeCp(CO)$_2$} (**8**), which has a similar structure as **3a**. If all *t*Bu substituents are replaced by *i*Pr groups, the chelate complex [*i*Pr$_2$P–P–P*i*Pr$_2$]{FeCp(CO)} (**6**) was formed, accompanied by spontaneous CO elimination. This shows that the type of the resulting complex can strongly be governed by the choice of the R substituents in the triphosphane ligand. Therefore, it is worth to carry out further investigations by varying the steric and electronic properties of the substituents of the P_3 unit.

Experimental Section

Experimental procedures and relevant characterization data of newly synthesized compounds can be found in the Supporting Information along with DFT calculation details and SC-XRD data.

Deposition Number(s) 2286589 (for **3a**), 2286590 (for **3b**), 2286591 (for **6**), and 2286592 (for **8**) contain(s) the supplementary crystallographic data for this paper. These data are provided free of charge by the joint Cambridge Crystallographic Data Centre and Fachinformationszentrum Karlsruhe Access Structures service.

Acknowledgements

Z. K. is grateful for the general support of János Bolyai Research Scholarship, Project UNKP-23-5 BME-419 and TKP2021-EGA-02 provided by the Ministry of Innovation and Technology of Hungary. T. H and P. B. are grateful for the National Research, Development and Innovation Office-NKFIH for the support through OTKA K146790 project. D.G. is grateful for the DCEP funded by the National Research Development and Innovation Fund of the Ministry of Culture and Innovation and the Budapest University of Technology and Economics, under a grant agreement with the National Research, Development and Innovation Office. We thank Prof. H. Schnöckel for the use of X-ray diffractometer.

Conflict of Interests

The authors declare no conflict of interest.

Data Availability Statement

The data that support the findings of this study are available in the supplementary material of this article.

Keywords: ligand effects · NMR spectroscopy · P ligand · transition metal complex · X-ray diffraction

[1] A. B. Burg, W. J. Mahler, *J. Am. Chem. Soc.* **1961**, *83*, 2388.
[2] S. Shah, J. D. Protasiewicz, *Coord. Chem. Rev.* **2000**, *210*, 181.
[3] a) G. Fritz, T. Vaahs, H. Fleischer, E. Matern, *Angew. Chem. Int. Ed.* **1989**, *28*, 315; b) I. Kovács, V. Balema, A. Bassowa, E. Matern, E. Sattler, G. Fritz, H. Borrmann, H. Bauernschmitt, R. Ahlrichs, *Z. Anorg. Allg. Chem.* **1994**, *620*, 2033.
[4] I. Kovács, E. Matern, G. Fritz, *Z. Anorg. Allg. Chem.* **1996**, *622*, 935.
[5] I. Kovács, G. Fritz, *Z. Anorg. Allg. Chem.* **1994**, *620*, 4.
[6] I. Kovács, E. Matern, E. Sattler, G. Fritz, *Z. Anorg. Allg. Chem.* **1996**, *622*, 1819.
[7] a) J. Olkowska-Oetzel, J. Pikies, *Appl. Organomet. Chem.* **2003**, *17*, 28; b) H. Krautscheid, E. Matern, J. Olkowska-Oetzel, J. Pikies, G. Fritz, *Z. Anorg. Allg. Chem.* **2001**, *627*, 999; c) I. Krossing, U. Englert, E. Matern, J. Olkowska-Oetzel, J. Pikies, G. Fritz, *Z. Anorg. Allg. Chem.* **2002**, *628*, 446.
[8] I. Kovács, H. Krautscheid, E. Matern, G. Fritz, J. Pikies, *Z. Anorg. Allg. Chem.* **1997**, *623*, 1088.
[9] a) E. Baum, E. Matern, A. Robaszkiewicz, J. Pikies, *Z. Anorg. Allg. Chem.* **2006**, *632*, 1073; b) A. Wiśniewska, K. Baranowska, R. Grubba, E. Matern, J. Pikies, *Z. Anorg. Allg. Chem.* **2010**, *636*, 1549.
[10] R. Grubba, A. Wiśniewska, Ł. Ponikiewski, M. Caporali, M. Peruzzini, J. Pikies, *Eur. J. Inorg. Chem.* **2014**, *2014*, 1811.
[11] R. Grubba, A. Ordyszewska, K. Kaniewska, Ł. Ponikiewski, J. Chojnacki, D. Gudat, J. Pikies, *Inorg. Chem.* **2015**, *54*, 8380.
[12] A. Wiśniewska, R. Grubba, Ł. Ponikiewski, M. Zauliczny, J. Pikies, *Dalton Trans.* **2018**, *47*, 10213.
[13] H. Nakazawa, W. E. Buhro, G. Bertrand, J. A. Gladysz, *Inorg. Chem.* **1984**, *23*, 3431.
[14] H. Schmidbaur, G. Blaschke, B. Zimmer-Gasser, U. Schubert, *Chem. Ber.* **1980**, *113*, 1612.
[15] a) G. Fritz, E. Matern, H. Krautscheid, R. Ahlrichs, J. W. Olkowska, J. Pikies, *Z. Anorg. Allg. Chem.* **1999**, *625*, 1604; b) G. Fritz, B. Mayer, E. Matern, *Z. Anorg. Allg. Chem.* **1992**, *607*, 19; c) G. Fritz, H. Goesmann, B. Mayer, *Z. Anorg. Allg. Chem.* **1992**, *607*, 26.
[16] D. E. C. Corbridge, *The Structural Chemistry of Phosphorus*, Elsevier, Amsterdam, p. 20.
[17] H. Borrmann, I. Kovács, G. Fritz, *Z. Anorg. Allg. Chem.* **1994**, *620*, 1818.

[18] The Cambridge Structural Databank's Conquest software (version 2022.3.0) found 16527 P–Fe distance hits. The histogram of P–Fe distances (Figure S22) shows an almost perfect normal distribution. However, at longer P–Fe distances, a slower flattening of the curve is observed, which distorts the normal distribution. The shortest and longest P–Fe distances found were 1.939 Å and 2.822 Å, respectively. The mean value is 2.248 Å, with a variance of 0.006 Å^2 and a standard deviation of 0.078 Å. The mean deviation is 0.054 Å. The lower and upper quantiles for the P–Fe distances are 2.201 Å and 2.272 Å, respectively.
[19] K.-O. Feldmann, R. Fröhlich, J. J. Weigand, *Chem. Commun.* **2012**, *48*, 4296.
[20] J. Rohonczy, D NMR Lineshape Analysis Software Manual, Version 1.1, Rev. 071103, TopSpin 3.5 NMR Software, Bruker BioSpin, Germany.
[21] I. Kovács, H. Krautscheid, E. Matern, E. Sattler, G. Fritz, W. Hönle, H. Borrmann, H. G. von Schnering, *Z. Anorg. Allg. Chem.* **1996**, *622*, 1564.
[22] G. Fritz, T. Vaahs, *Z. Anorg. Allg. Chem.* **1987**, *552*, 18.
[23] I. Kovács, H. Krautscheid, E. Matern, G. Fritz, *Z. Anorg. Allg. Chem.* **1994**, *620*, 1369.
[24] B. F. Hallam, P. L. Pauson, *J. Chem. Soc.* **1956**, 3030.
[25] J. S. Plotkin, S. G. Shore, *Inorg. Chem.* **1981**, *20*, 284.
[26] CrystalClear SM 1.4.0 Rigaku/MSC Inc., 2008.
[27] NUMABS: T. Higashi, (1998), rev. 2002. (Rigaku/MSC Inc.).
[28] G. M. Sheldrick, *Acta Crystallogr.* **2008**, *A64*, 112.
[29] G. M. Sheldrick, *Acta Crystallogr.* **2015**, *C71*, 3.
[30] L. J. Farrugia, *J. Appl. Crystallogr.* **2012**, *45*, 849.
[31] A. L. Spek, *Acta Crystallogr.* **2009**, *D65*, 148.
[32] O. V. Dolomanov, L. J. Bourhis, R. J. Gildea, J. A. K. Howard, H. Puschmann, *J. Appl. Crystallogr.* **2009**, *42*, 339.
[33] C. F. Macrae, P. R. Edgington, P. McCabe, E. Pidcock, G. P. Shields, R. Taylor, M. Towler, J. van de Streek, *J. Appl. Crystallogr.* **2006**, *39*, 453.
[34] M. A. Spackman, D. Jayatilaka, *CrystEngComm.* **2009**, *11*, 19–32.
[35] M. J. Frisch, G. W. Trucks, H. B. Schlegel, G. E. Scuseria, M. A. Robb, J. R. Cheeseman, G. Scalmani, V. Barone, G. A. Petersson, H. Nakatsuji, X. Li, M. Caricato, A. V. Marenich, J. Bloino, B. G. Janesko, R. Gomperts, B. Mennucci, H. P. Hratchian, J. V. Ortiz, A. F. Izmaylov, J. L. Sonnenberg, Williams, F. Ding, F. Lipparini, F. Egidi, J. Goings, B. Peng, A. Petrone, T. Henderson, D. Ranasinghe, V. G. Zakrzewski, J. Gao, N. Rega, G. Zheng, W. Liang, M. Hada, M. Ehara, K. Toyota, R. Fukuda, J. Hasegawa, M. Ishida, T. Nakajima, Y. Honda, O. Kitao, H. Nakai, T. Vreven, K. Throssell, J. A. Montgomery Jr., J. E. Peralta, F. Ogliaro, M. J. Bearpark, J. J. Heyd, E. N. Brothers, K. N. Kudin, V. N. Staroverov, T. A. Keith, R. Kobayashi, J. Normand, K. Raghavachari, A. P. Rendell, J. C. Burant, S. S. Iyengar, J. Tomasi, M. Cossi, J. M. Millam, M. Klene, C. Adamo, R. Cammi, J. W. Ochterski, R. L. Martin, K. Morokuma, O. Farkas, J. B. Foresman, D. J. Fox, Gaussian 16 Rev. C.01, Wallingford, CT, **2016**. 12.
[36] T. Lu, F. Chen, *J. Comput. Chem.* **2012**, *33*, 580.
[37] A. T. B. Gilbert, IQmol molecular viewer. Available at: http://iqmol.org (Accessed October, **2012**).

Manuscript received: August 15, 2023
Accepted manuscript online: October 7, 2023
Version of record online: ■■, ■■

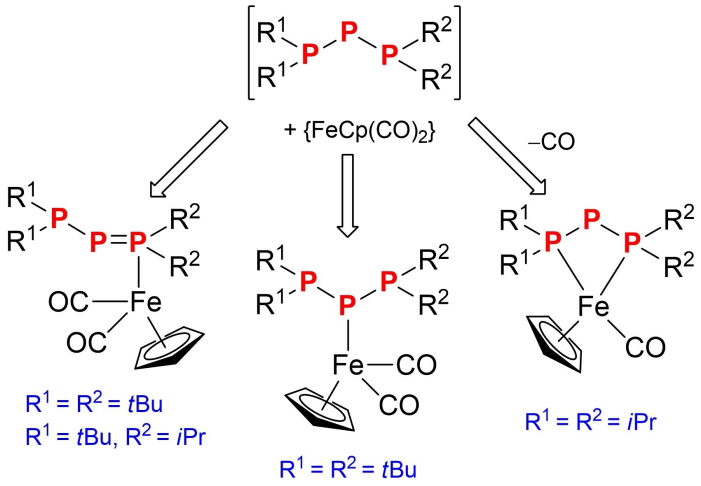

Dr. T. Holczbauer, D. Gál, Dr. J. Rohonczy, Dr. E. Matern, Dr. E. Sattler, Dr. P. Bombicz, Dr. Z. Kelemen, Dr. I. Kovács**

1 – 9

Iron(II) Complexes of P_3-Chain Ligands: Structural Diversity

Iron(II) complexes containing a $R_2P–P–PR_2$ unit were synthetized. The binding modes of the triphosphane ligands can be changed by the size of the substituents. The products were characterized by NMR spectroscopy and single-crystal X-ray diffraction.